Evaluation of regularization approaches in electrocardiographic imaging problem

Vojko Jazbinšek[1], Matija Milanič[2], Rok Hren[1]

[1]Institute of Mathematics, Physics and Mechanics, Ljubljana, Slovenia; [2]J. Stefan Institute, Ljubljana, Slovenia

Motivation: To compare various regularization techniques using the same volume conductor and cardiac source models.

ECGI problem

Electrocardiographic imaging (ECGI) [1-5] is a method of computing potentials on the epicardium Φ_E from measured or simulated potentials on the torso surface Φ_T

Forward: $\Phi_T = \mathbf{A}\,\Phi_E$ (BEM, FEM)

Inverse: $\Phi_E = \mathbf{A}^{-1}\,\Phi_T$

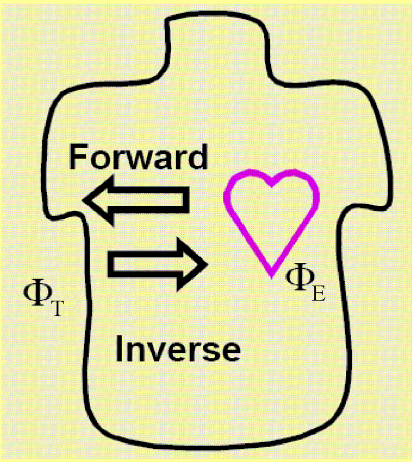

The matrix $\mathbf{A}$ is ill-conditioned and regularization is needed for obtaining stable inverse solution.

We analyzed 14 regularization techniques summarized in (Table 1), which we organized in 3 groups

A – Tikhonov-based methods: $\min_{\Phi_T} \{ \| \Phi_T - \mathbf{A}\,\Phi_E \|_2 + \lambda^2 \| \boldsymbol{\Lambda}\,\Phi_E \|_2 \}$

B – Iterative methods

C – Non-quadratic methods : $\min_{\Phi_T} \{ \| \Phi_T - \mathbf{A}\,\Phi_E \|_2 + \lambda^2 \| \boldsymbol{\Lambda}\,\Phi_E \|_1 \}$

λ – regularization parameter, $\boldsymbol{\Lambda}$ – regularization operator ($Z=\mathbf{I}$, $F=\mathbf{G}$, $S=\mathbf{L}$)

Protocol

Step 1: Measurements at CVRTI* - Electric potentials were recorded from the 602-lead cylindrical cage enveloping the suspended canine heart and thus serving as the "epicardial" surface (ϕ_E^m), see Fig. 1.

Step 2: Calculation of torso potentials at 771 nodes using BEM and FEM*. Three noise levels (20 dB, 40 dB, 60 dB) were added to the torso potentials to mimic experimental measurement conditions.

Step 3. The 602-lead cylindrical cage potentials were reconstructed by the 14 regularization techniques, summarized in Table 1,

Step 4: We expressed the accuracy of the inverse solution (ϕ_E^c) in terms of

$$RE = \left\| \phi_E^c - \phi_E^m \right\|_2 \Big/ \left\| \phi_E^m \right\|_2, \quad CC = \phi_E^c \cdot \phi_E^m \Big/ \left\| \phi_E^c \right\|_2 \left\| \phi_E^m \right\|_2$$

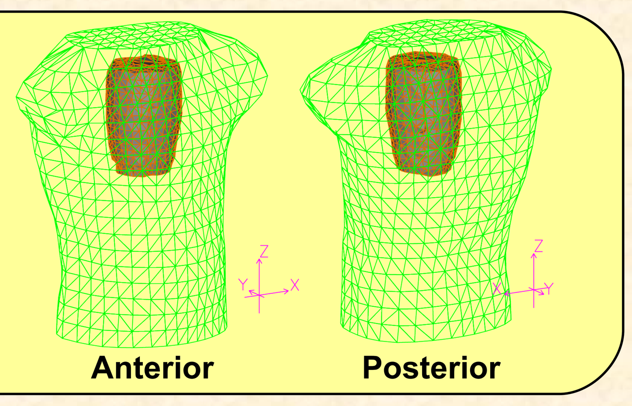

Fig. 1: Anterior and posterior views of the torso and cage surfaces. Cage with the heart was positioned inside an electrolytic tank shaped like an adolescent thorax. Data recorded during normal sinus rhythm at 602 leads of the cylindrical cage were used to compute torso potentials at 771 nodes using BEM and FEM*.

Table 1: Summary of 14 regularization techiques subdivided into 3 groups

Group	Acronym	Short description	Reference
A	ZOT	Zero-order Tikhonov	[6,7]
	FOT	First-order Tikhonov	[4]
	SOT	Second-order Tikhonov	[7]
B	ZCG	Zero-order Conjugate Gradient	[8]
	FCG	First-order Conjugate Gradient	[8]
	SCG	Second-order Conjugate Gradient	[8]
	ZLSQR	Zero-order LSQR	[9]
	FLSQR	First-order LSQR	[9]
	SLSQR	Second-order LSQR	[9]
	TSVD	Truncated Singular Value decomposition	[10]
	ν	ν-method	[10]
C	FTV	Total variation	[2,4]
	STV	Total variation with Laplacian	[2,4]
	LASSO	Least Absolute Selection and Shrinking Operator	[11]

References

[1] Oster HS, Taccardi B, Lux RL, Ershler PR Rudy Y. Noninvasive electrocardiographic imaging: Reconstruction of epicardial potentials, electrograms, isochrones and localization of single and multiple electrocardiac events. Circulation 1997, 96: 1012-1024.

[2] Rudy Y, Messinger-Rapport BJ. The inverse problem in electrocardiography: Solutions in terms of epicardial potentials. CRC Crit. Rev. Biomed. Eng. 16: 215-268.

[3] Hren R. Value of epicardial potential maps in localizing pre-excitation sites for radiofrequency ablation. A simulation study. Phys. Med. Biol. 1998, 43:1449-1468.

[4] Ghosh S, Rudy Y. Application of L1-norm regularization to epicardial potential solution of the inverse electrocardiography problem. Ann. Biomed. Eng. 2009, 37: 902-912.

[5] Horacek BM, Clements JC. The inverse problem of electrocardiography: a solution in terms of single- and double-layer sources of the epicardial surface. Math Biosci 1997, 144: 119-154.

[6] Tikhonov A, Arsenin V. Solution of Ill-Posed Problems. Washington, DC: Winston, 1977.

[7] Brooks DH, Ghandi FA, MacLeod RS. Inverse electrocardiography by simultaneous imposition of multiple constraints, IEEE Trans. Biomed. Eng. 1999, 46: 3-18.

[8] Hanke M. Conjugate Gradient Type Methods for Ill-Posed Problems. Harlow: Longman Scientific & Technical, 1995.

[9] Paige CC, Saunders MA. LSQR: An algorithm for sparse linear equations and sparse least squares, ACM Transactions on Mathematical Software 1982, 8: 43-71.

[10] Hansen PC. Rank-Deficient and Discrete Ill-Posed Problems. Philadelphia: SIAM, 1998.

[11] Schmidt M. Least Squares Optimization with L1-Norm Regularization, Project Report , University of British Columbia, 2005

Results – Initial phase of the QRS complex

Table 2: Relative errors (RE) for reconstruction results at 5 (Q_5), 10 (Q_{10}), 15 (Q_{15}) ms after the Q-onset; Q_{pk} refers to the distributions at the peak of the Q-wave.

	ZOT	FOT	SOT	ZCG	FCG	SCG	ZLSQR	FLSQR	SLSQR	TSVD	ν	FTV	STV	LASSO
Q_5	0.32	0.22	0.22	0.32	0.25	0.25	0.32	0.25	0.25	0.33	0.32	0.23	0.22	0.36
Q_{10}	0.26	0.11	0.10	0.26	0.11	0.11	0.26	0.11	0.11	0.27	0.26	0.15	0.12	0.26
Q_{15}	0.30	0.18	0.16	0.26	0.19	0.15	0.26	0.19	0.15	0.27	0.27	0.14	0.13	0.27
Q_{pk}	0.49	0.43	0.39	0.40	0.45	0.38	0.40	0.45	0.38	0.44	0.45	0.31	0.25	0.40

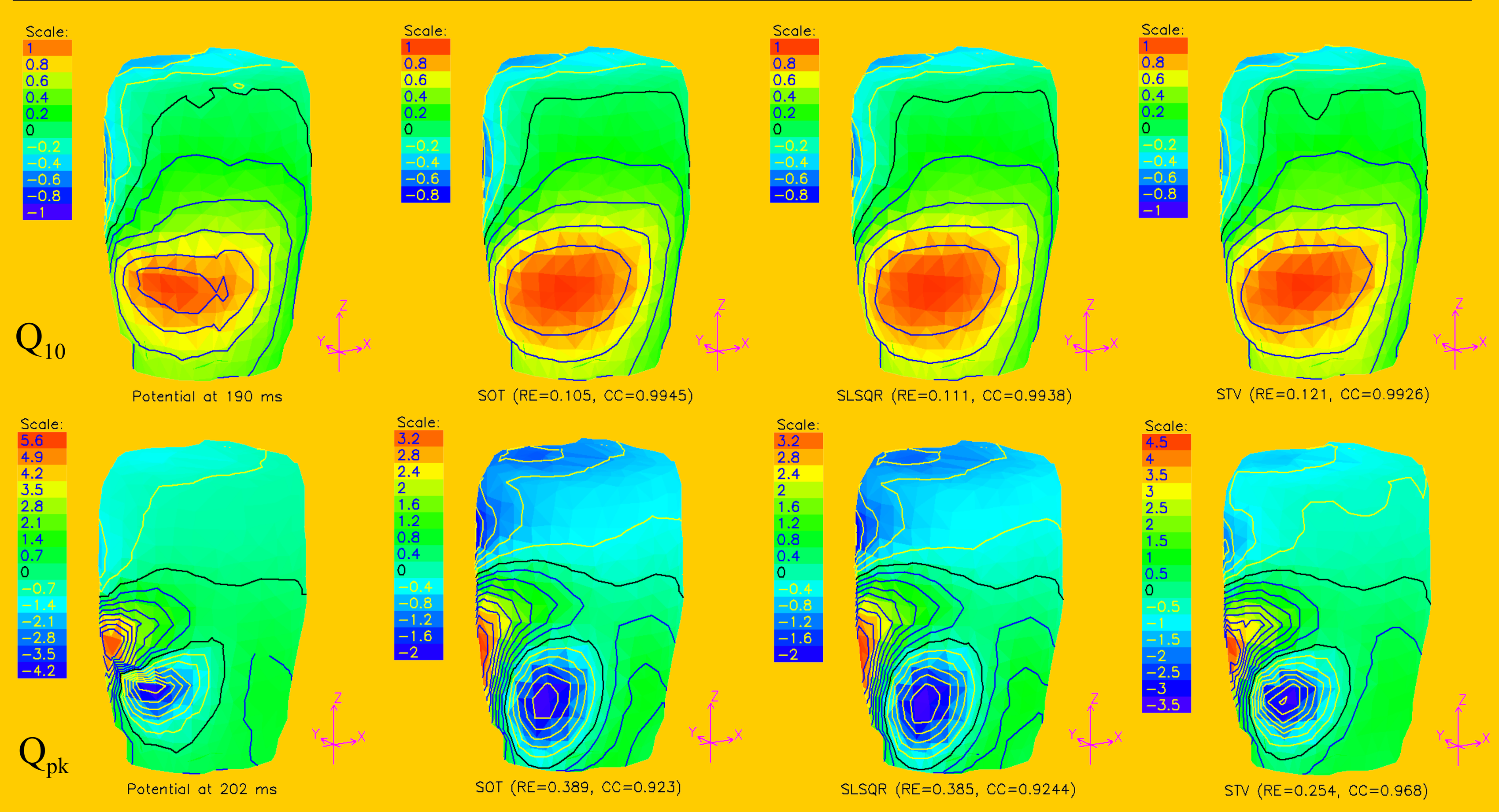

Fig 2: Measured and reconstructed potential distributions using SOT, SLSQR and STV regularization techniques at 10 (Q_{10}) ms after the Q-onset and at the peak (Q_{pk}) of the Q-wave.

Results – standard reference points (P,R,S,T)

Table 3. Relative errors (RE) for reconstruction results at standard reference points of the sinus rhythm (peaks of P, R, S, and T waves) in the presence of a 40-db noise and when using BEM.

	ZOT	FOT	SOT	ZCG	FCG	SCG	ZLSQR	FLSQR	SLSQR	TSVD	ν	FTV	STV	LASSO
P	0.47	0.43	0.42	0.47	0.45	0.45	0.47	0.45	0.45	0.51	0.48	0.37	0.41	0.45
R	0.45	0.40	0.39	0.40	0.40	0.38	0.40	0.40	0.38	0.42	0.43	0.35	0.33	0.40
S	0.48	0.42	0.40	0.47	0.45	0.44	0.47	0.45	0.44	0.50	0.49	0.37	0.40	0.45
T	0.27	0.16	0.16	0.26	0.16	0.16	0.26	0.16	0.16	0.27	0.26	0.17	0.16	0.26

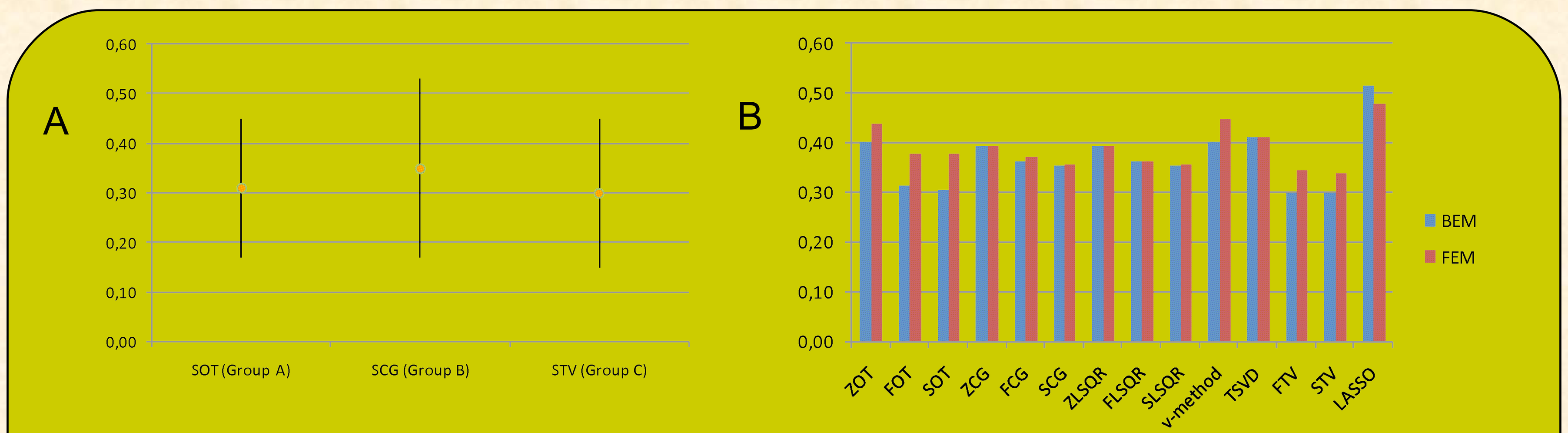

Fig 3: A – Average RE (±SD) over the entire sinus rhythm (n=484) for SOT (Group A), SCG (Group B) and STV (group C). B – comparison of average RE when using BEM and FEM forward calculations.

Conclusions

- Total variation methods (FTV,STV) appears most robust (see, results in Tables 2,3 and Figs. 2-4),
- Second-order operators appear to better capture complex spatial patterns,
- For isotropic and homogeneous volume conductor, BEM is superior to FEM (Fig. 3B).

Future work:

- Identification of early activation sites during pacing and in the circumstances of infarcted hearts
- Evaluation of approaches to regularizing biomagnetic inverse problem (minimum norm estimates).

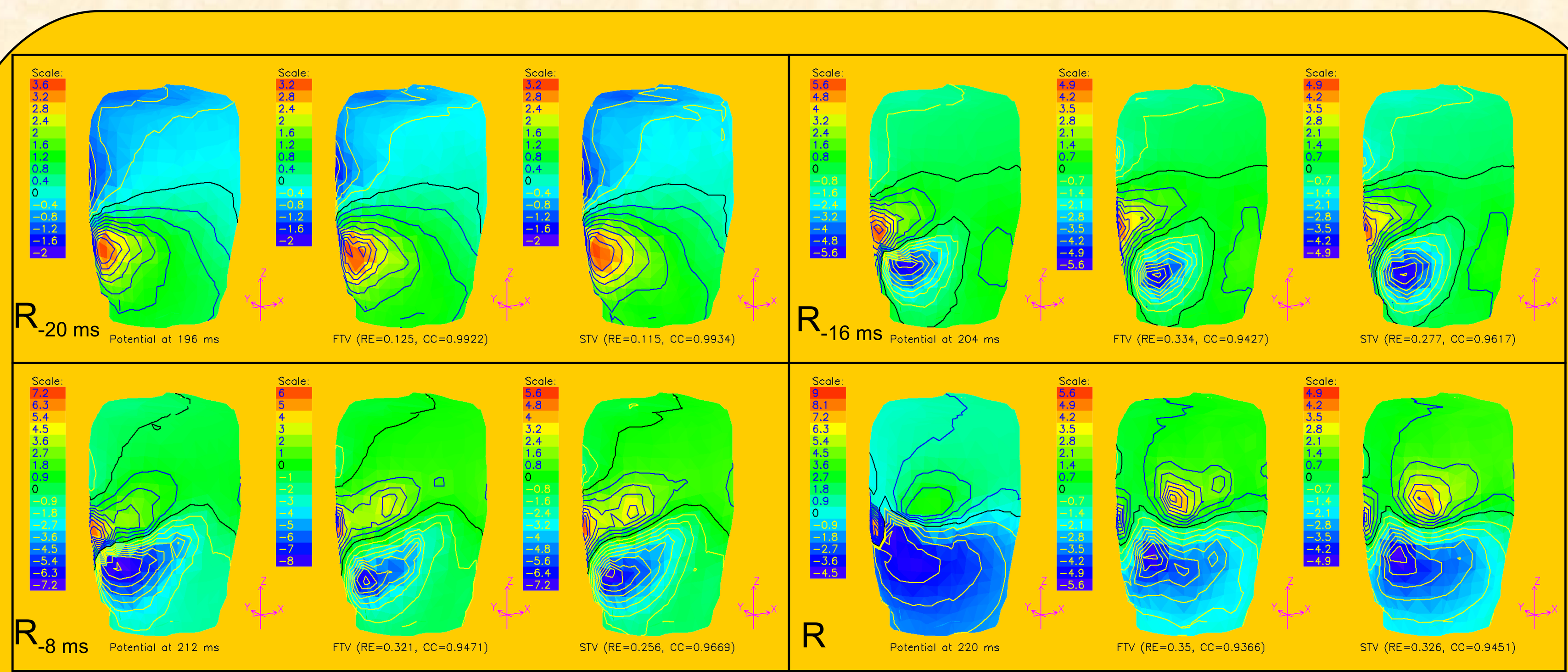

Fig 4: Measured and reconstructed potential distributions using FTV and STV regularization techniques in Q-R interval in steps of 8 ms (at R-20, R-16, R-8 ms, and at R peak).

***Acknowledgment**

We thank R.S. MacLeod from CVRTI, Salt Lake City, UT, USA for the measured data, and D.F. Wang from Scientific Computing and Imaging Institute, University of Utah, Salt Lake City, UT, USA for FEM forward data.